

Complex Fluid Static Property
(Current Research on Static Property of Complex Fluid in Confined Micro-Spaces)

1. Complex Fluids

(complex fluid) , (macromolecule) 가
 (polyelectrolyte) , biofluid 가
 (simple fluid) . Complex fluid
 Table 1 [1,2].
 , complex fluid ,
 i) molecular length scale microstructural .
 ii) long-range interaction . , long-range
 interaction physicochemical interaction Lennard-Jones(LJ), repulsion, attraction
 [3].
 iii) . 가
 many-body interaction [4].

Table 1. Classification of complex fluids.

microstructures of complex fluid particles		example
(spherical) 	Rigid	latex, microspheres
	Deformable	emulsion, micelle
- (axisymmetric-nonspherical) 	Ellipsoidal Spheroid	(albumin, globulin)
	Prolate	clay , silt
	Rod-like	DNA, , ,
(chain structure) 	Semi-flexible	가 (polyelectrolyte), (brushed & tethered), (polysaccharide),
	Flexible	

2. Complex Fluids in Confined Micro-Spaces

Complex fluid (confined space) , Fig 1 slit-like pore cylindrical pore well-defined structure disordered porous fibrous geometry heterogeneous structure [5,6].

Table 2 confined complex fluid (unbounded space) complex fluid hydrodynamic interaction non-hydrodynamic interaction 가

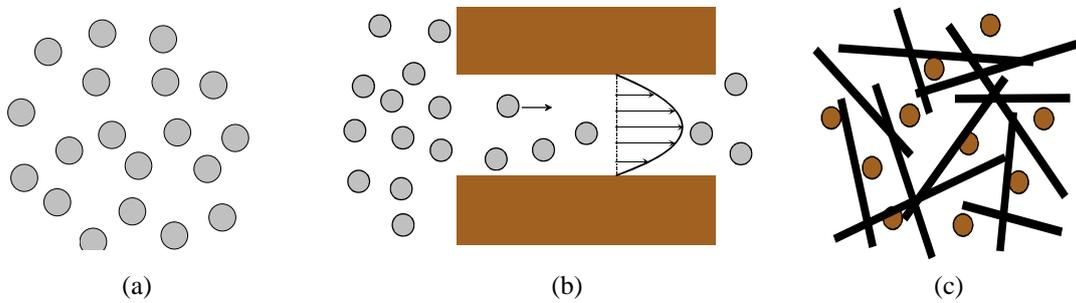


Fig. 1. Complex fluids in (a) unbounded space, (b) confined space of micro-channel, and (c) confined spaces of disordered fibrous media.

Table 2. Complex Fluids Processing Micro-Fluidics Aspects.

Focused areas	Complex fluids processing	Micro-fluidics aspects
	capillary gel electrophoresis fields flow fractionation	Hindered diffusion, convection, electrostatic interaction, electroosmosis, electrokinetic flow, Taylor dispersion, concentration partitioning
Bio & Medical	Bio-Chip (DNA-chip, Lab-on-a-chip)	Diffusion, electrostatic interaction, flow and rheological aspects of blood, ion transport
	(super-molecules) mesoporous	Particle-particle interaction, hindered diffusion, size exclusion, inter- & intra-pore interaction

3. Static Properties

3.1. Radial density distribution of colloidal suspension

(equilibrium partitioning) [7,8]. r

R ratio C_p C

(partition coefficient) $K(= C_p/C_b)$

$$K = \frac{\int_0^{1-\lambda} C(\beta) \beta d\beta}{\int_0^1 C(\beta) \beta d\beta}$$

$\lambda = r/R$, β dimensionless radial distance, $C(\beta)$

long-range $E(\beta)$

$C(\beta) = \exp(-E(\beta)/kT)$

- long-range interaction 가

radial density distribution

Gibbs ensemble Monte Carlo (GEMC)

[9,10]. GEMC virial expansion density functional 가

Stochastic process GEMC canonical (NVT), isobaric-isothermal (NPT), grand canonical (μVT) ensemble, Fig. 2

NPT (periodic boundary condition) (random displacement) NVT

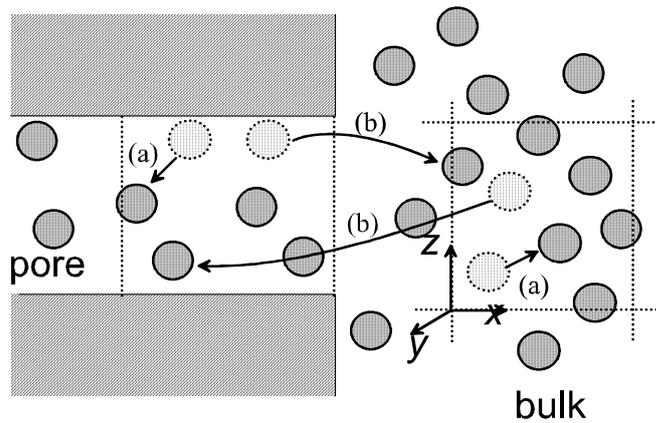


Fig. 2. GEMC method for the simulation of equilibrium partitioning, (a) random displacements, (b) particle interchange between two regions[9].

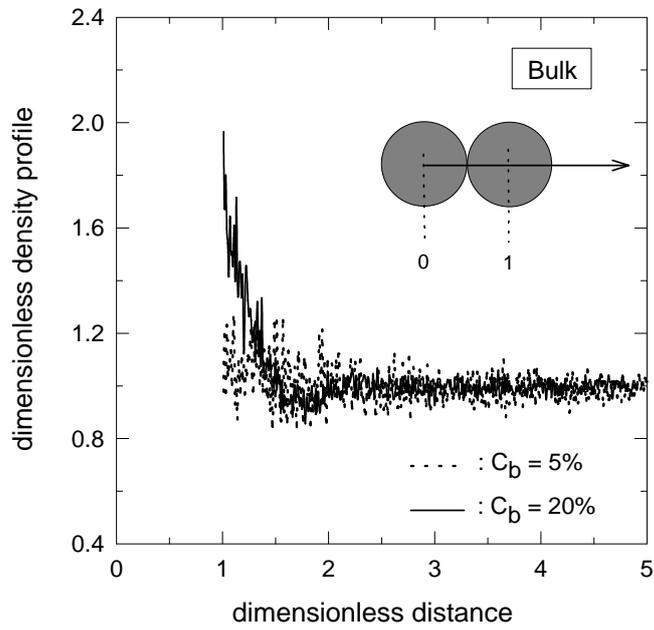
process (interchange) μVT process
 ensemble $\exp(-E^\alpha/kT)$
 configuration (500~1300)
 adjust parameter
 configuration
 , pair-wise additive

Fig. 3

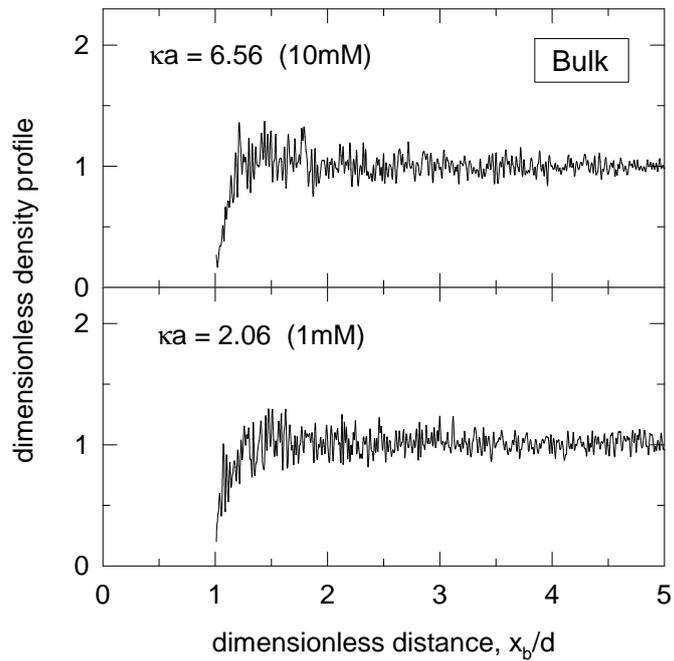
(radial distribution function) [2,11].

(depletion)
 Infinite dilute (100~0.1mM)
 가 가 Fig. 4
 GEMC virial expansion 가
 가 가 ,
 가 가
 가 virial expansion λ
 가 가
 (, $\lambda > 0.5$) 가 가 ,

GEMC Happel Brenner[12] centerline
 approximation 가
 , fibrous media disordered fiber
 radial density distribution 가 [13,14]. fiber
 fiber 가 (3 Vol %) , Fig. 5 fiber
 simulation cell GEMC [14]. Fig. 6 fiber
 가 1 Vol %, fiber 가 1, 가 1 10 Vol %
 , ionic strength dimensionless inverse Debye length ($= \kappa r_p$)
 radial density distribution . Debye length 가 , κr_p fiber



(a)



(b)

Fig. 3. (a) Density profiles of spherical solutes in the bulk for uncharged case and solute concentrations of 5 and 20 Vol %, (b) Density profiles of charged solutes in the bulk for $\kappa a = 6.56$ and 2.06 (ionic strength = 10 and 1 mM), and solute concentrations of 5.2 Vol %.

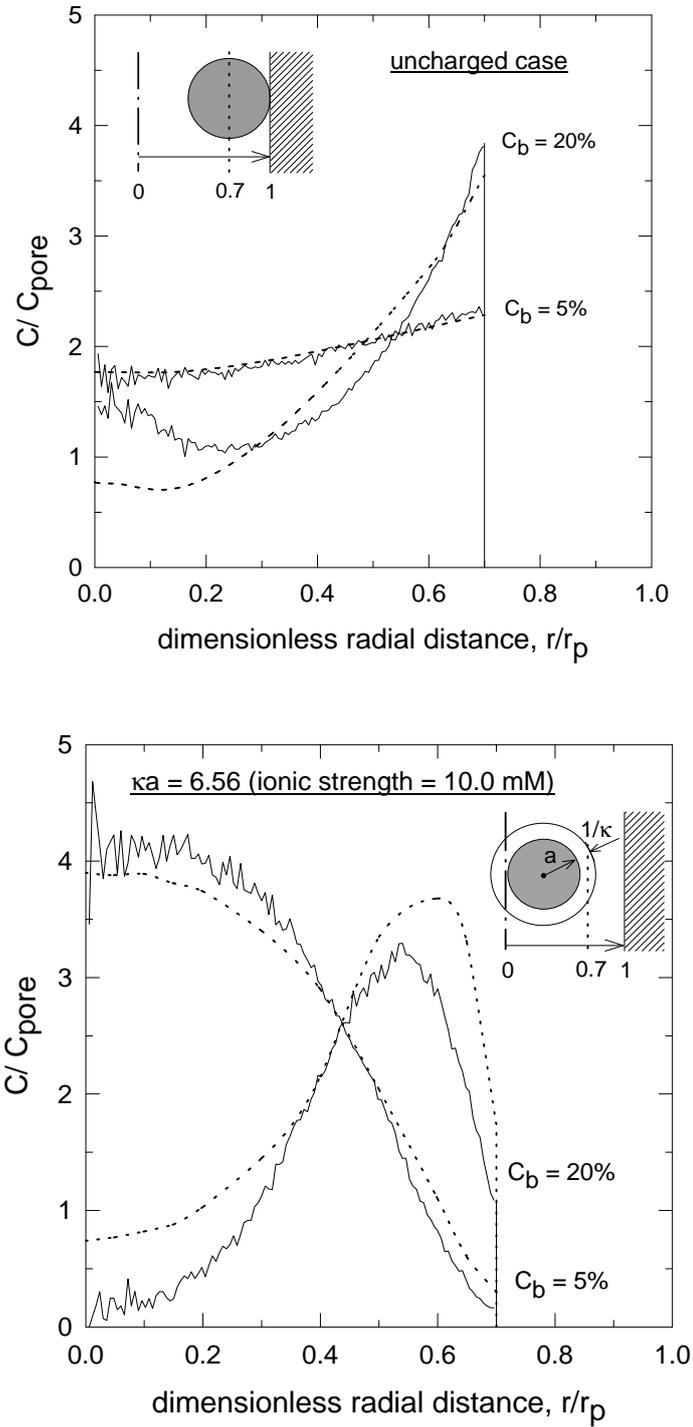


Fig. 4. Density profiles of uncharged solutes and charged solutes in the cylindrical pore for $\kappa a = 6.56$ (i.e., ionic strength = 10mM), $\lambda = 0.3$ and solute concentrations of 5 and 20 Vol %. Dotted curves correspond to virial expansion results.

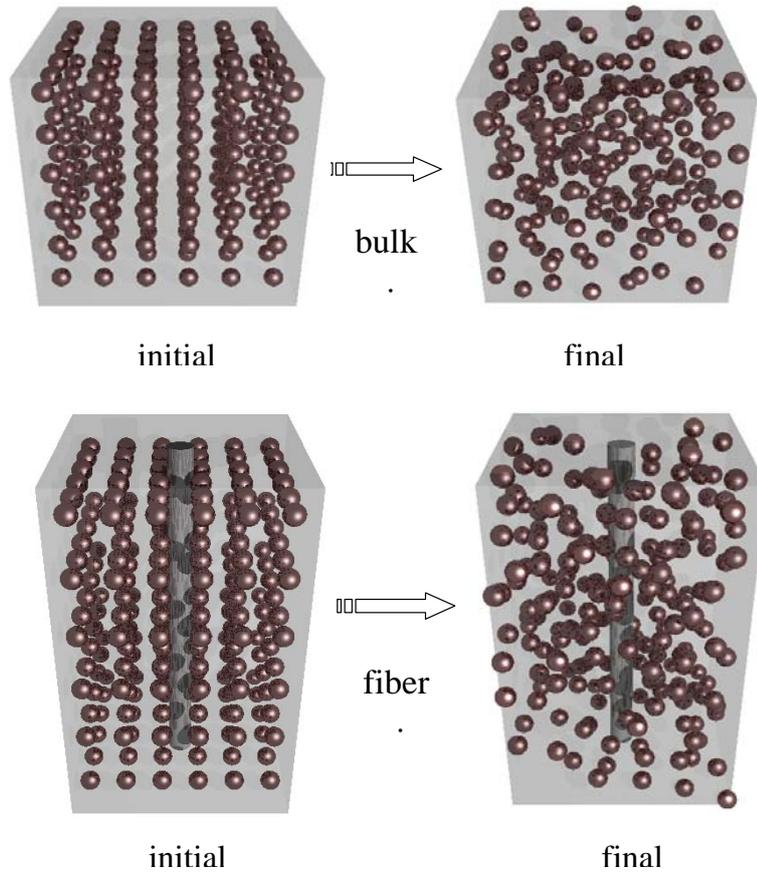


Fig. 5. Snapshots of particles in both the bulk and the fiber regions by performing of GEMC simulation for charged system with $\lambda = 1.0$, $\phi_f = 0.01$, and particle concentration of 10 Vol %.

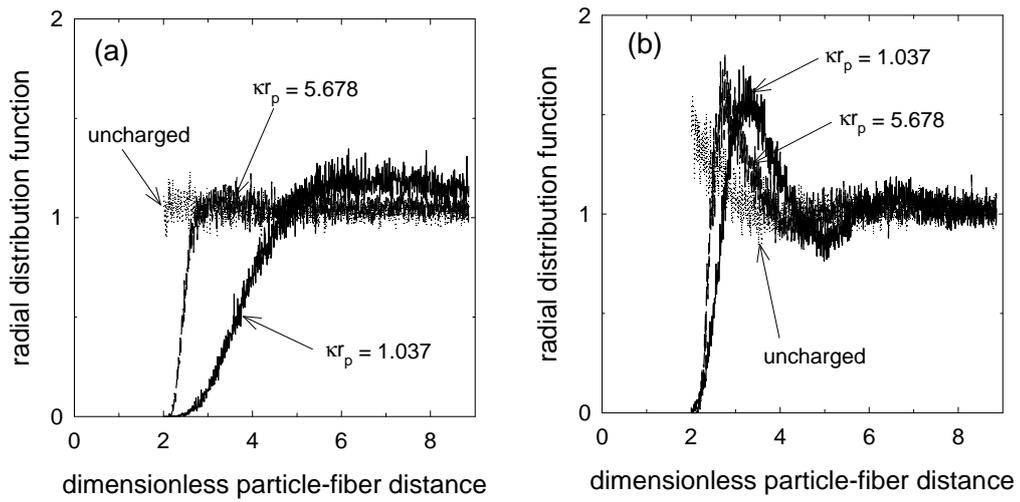


Fig. 6. Comparison of radial density profiles of particles around a fiber with different electrostatic interactions for $\lambda = 1.0$ and several particle concentrations C_p of (a) 1 and (b) 10 Vol %.

3.2. Conformational Property of Polyelectrolyte Solution

(1) Monte Carlo (MC) and Molecular Dynamics (MD) Simulation

Max-Planck Institute for Polymer Research, Theory Group Kremer, (MD)
flexible polyelectrolyte overlap concentration
well-defined peak χ scattering function [15].
peak (density correlation)
, NVT MC uncharged highly charged polyelectrolyte
[6]. , semidilute
density oscillation
density oscillation , poor backbone solubility, counterion
segment-segment electrostatic interaction , weakly charged
single flexible polyelectrolyte heat bath MC velocity Verlet MD
. MC , off-lattice
pivot
conformational space [16,17].
Charged polyelectrolyte long-range interaction
polyelectrolyte crossover χ polymer density (,
monomer density) . good solvent, poor solvent
salt χ
polyelectrolyte
polyelectrolyte
 χ hybrid MD+MC

(2) Chain Conformation

Rodlike polyelectrolyte rod orientational order χ ,
flexible polyelectrolyte . MPIP Micka
[18] flexible polyelectrolyte MD ,
radius of gyration, end-to-end distance, structure factor, scaling property
. N monomer flexible polyelectrolyte Lennard-
Jones(LJ) bead-spring chain . χ monomer
neutral Kuhn step harmonic spring random walk χ .
MD (kT = 1.0 ϵ) damping constant time step Langevin
thermoset . monomer screened Coulomb potential

counterion screening Poisson-Boltzmann Bjerrum length λ_B electrostatic energy Boltzmann thermal energy kT Debye-Hückel persistence length λ_p inverse Debye length κ

Figs. 7 8 polymer density necklace-like polymer density (collapsed agglomeration Polymer density λ_p λ_p crossover

polyelectrolyte conformation λ_p monomer bond length l persistence length λ_p N-monomer chain end-to-end distance R_{end} radius of gyration R_g [19].

$$\langle R_{end}^2 \rangle = \langle (\mathbf{r}_N - \mathbf{r}_1)^2 \rangle = l^2 (N-1)$$

$$\langle R_g^2 \rangle = \frac{1}{N} \left\langle \sum_{i=1}^N (\mathbf{r}_i - \mathbf{r}_{cm})^2 \right\rangle = \frac{l^2 (N-1)}{6}$$

, $\mathbf{r}_N, \mathbf{r}_1$ chain-end, \mathbf{r}_{cm} chain center of mass $1/N (\sum \mathbf{r}_i)$ Fig. 9 chain structure factor \mathbf{q} [19,20].

$$S(\mathbf{q}) = \left\langle \frac{1}{N} \left| \sum_{i,j} \exp(-i\mathbf{q} \cdot (\mathbf{r}_i - \mathbf{r}_j)) \right|^2 \right\rangle$$

, q wavenumber, $S(\mathbf{q})$ pair correlation function Fourier transformation scaling law

$$\langle R_{end}^2 \rangle \propto \langle R_g^2 \rangle \propto N^{2\nu}$$

, $\nu = 0.588$ self-avoiding walk expanding good solvent, $\nu = 1/2$ random walk repulsion attraction θ solvent, $\nu = 1/3$ collapsed poor solvent, coil-to-rodlike structure transition characteristic ratio

$$r = \frac{R_{end}^2}{R_g^2}$$

, rodlike limit $r = 12$, flexible chain in good solvent $r \approx 6.3$, ideal chain (, random walk) $r = 6$

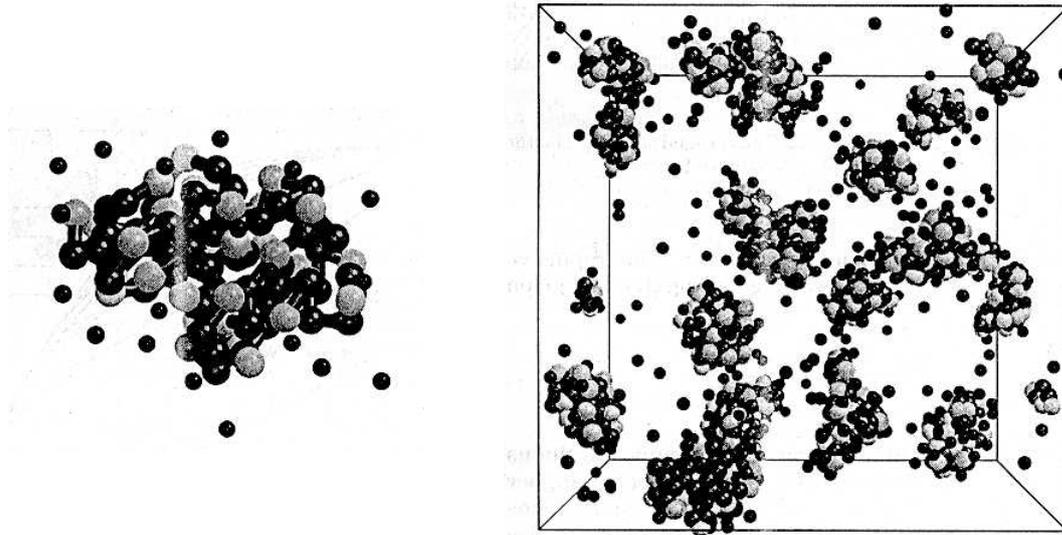


Fig. 7. Conformations at the density $\rho = 2 \times 10^{-2} \sigma^{-3}$. left: typical poor solvent polyelectrolyte conformation. The light-colored beads are the charged monomers, the counterions are indicated as small black spheres, and the neutral monomers are dark gray spheres. Only counterions within a distance of 3σ to the chain are displayed. right: snapshot of the whole simulation box, showing all 16 chains together with their counterions. The picture shows that the chains collapse into single globules that are well separated, and a small fraction of the counterions is still in solution[18].

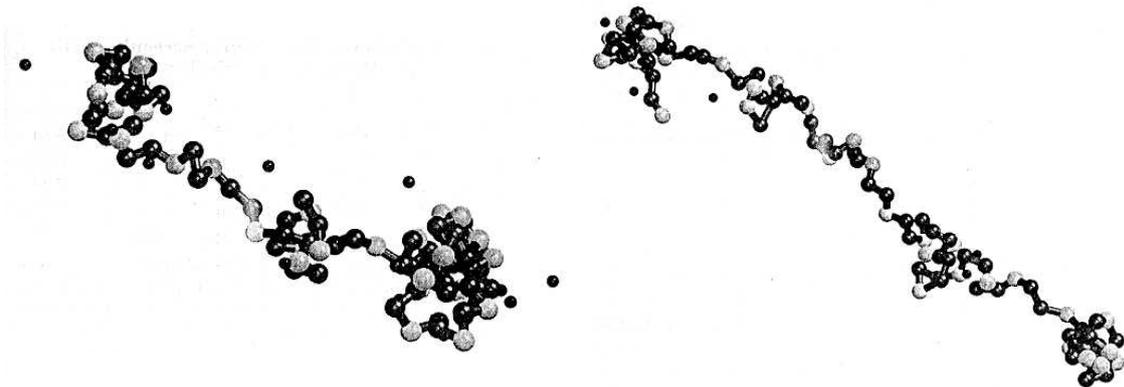


Fig. 8. Typical poor solvent polyelectrolyte conformation, (left) for the density $\rho = 2 \times 10^{-5} \sigma^{-3}$, which shows nicely a pearl-necklace structure, (right) for the density $\rho = 2 \times 10^{-6} \sigma^{-3}$, showing a very elongated, but still pearl-necklace structure[18].

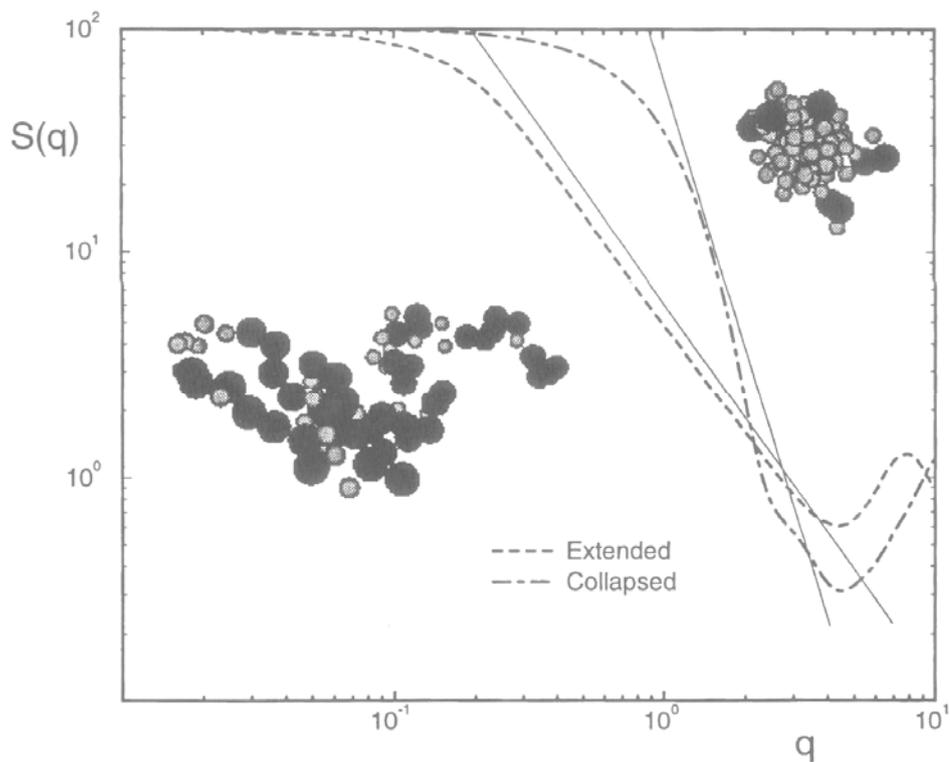


Fig. 9. Static structure function for $N = 100$ at the collapse transition point for the simple polyelectrolyte model. The bigger spheres denote the “popped” (hydrogen bonded) monomers. For the expanded part the popped monomers are equally distributed all over the chain, while for the collapsed system only a few sites remain available to build up a solvation shell. The asymptotic slopes for the two cases of $q^{-1/0.588}$ and q^{-4} respectively are indicated by straight lines[19].

4.

- (1) Larson, R.G., *The Structure and Rheology of Complex Fluids*, Oxford Univ. Press, NY (1999).
- (2) Russel, W.B., Saville, D.A. and Schowalter, W.R., *Colloidal Dispersions*, Cambridge Univ. Press, NY (1989).
- (3) Israelachvili, J.N., *Intermolecular and Surface Forces: With Applications to Colloidal and Biological Systems*, Academic Press, San Diego (1985).
- (4) Allen, M.P. and Tildesley, D.J., *Computer Simulation of Liquids*, Oxford Univ. Press, New York (1987).
- (5) Deen, W.M., “Hindered Transport of Large Molecules in Liquid-Filled Pores”, *AIChE J.*, **33**, 1409 (1987).
- (6) Carignano, M.A. and Dan, N., “Density Inhomogeneities of Highly Charged Polyelectrolyte Solutions

- Confined between Uncharged and Nonadsorbing Walls”, *Langmuir*, **14**, 3475 (1998).
- (7) Davidson, M.G., Suter, U.W. and Deen, W.M., “Equilibrium Partitioning of Flexible Macromolecules between Bulk Solution and Cylindrical Pores”, *Macromolecules*, **20**, 1141 (1987).
- (8) Lin, N.P. and Deen, W.M., “Effects of Long-Range Polymer-Pore Interactions on the Partitioning of Linear Polymers”, *Macromolecules*, **23**, 2947 (1990).
- (9) Chun, M.-S. and Phillips, R.J., "Electrostatic Partitioning in Slit-Pores by Gibbs Ensemble Monte Carlo Simulation", *AIChE J.*, **43**, 1194 (1997).
- (10) Chun, M.-S., "Computer simulation study on the concentration distribution of spherical colloids within confined spaces of well-defined pores", *Macromolecular Theory Simulations*, **8**, 418 (1999).
- (11) Sadus, R.J., *Molecular Simulation of Fluids: Theory, Algorithms and Object-Oriented*, Elsevier, Amsterdam (1999).
- (12) Happel, J. and Brenner, H., *Low Reynolds Number Hydrodynamics: with special applications to particulate media*, Martinus Nijhoff, The Hague (1983).
- (13) White, J.A. and Deen, W.M., “Equilibrium partitioning of flexible macromolecules in fibrous membranes and gels”, *Macromolecules*, **33**, 8504 (2000).
- (14) Chun, M.-S. and Baig, C.K., “Molecular Simulation Study on the Colloidal Suspension Within Dilute Fibrous Media: The Effect of Particle Concentration on Partitioning“, *Korean J. Chem. Eng.*, in press (2001).
- (15) Stevens, M.J. and Kremer, K., “Structure of Salt-Free Linear Polyelectrolytes in the Debye-Hckel Approximation”, *J. Phys. II France*, **6**, 1607 (1996).
- (16) Micka, U. and Kremer, K., “Persistence length of the Debye-Hckel model of weakly charged flexible polyelectrolyte chains”, *Phys. Rev. E*, **54**, 2653 (1996).
- (17) Micka, U. and Kremer, K., “Persistence length of weakly charged polyelectrolytes with variable intrinsic stiffness”, *Europhys. Lett.*, **38**, 279 (1997).
- (18) Micka, U., Holm, C. and Kremer, K., “Strongly Charged, Flexible Polyelectrolytes in Poor Solvents: Molecular Dynamics Simulations”, *Langmuir*, **15**, 4033 (1999).
- (19) Binder, K. and Ciccotti, G. (Eds.), *Monte Carlo and Molecular Dynamics of Condensed Matter Systems*, Societa Italiana Di Fisica, Bologna (1996).
- (20) van de Ven, T.G.M., *Colloidal Hydrodynamics*, Academic Press, London (1989).